Towards a Mechatronic Compiler

Hendrik Van Brussel, *Fellow, IEEE*, Paul Sas, István Németh, Pierre De Fonseca, and Pieter Van den Braembussche

***Abstract*—A simultaneous engineering framework for designing optimal mechatronic systems is presented. In the first part of this paper, a method, based on genetic algorithms, for optimizing the geometric configuration of three-axis machine tools in the conceptual design stage is presented. The second part describes a method, based on component mode synthesis, to derive a low-order control model from a finite-element description of the mechanial and drive structures of the mechatronic system. In the third part, motion controllers are derived that are robust against configuration changes of the mechatronic system to be controlled.**

***Index Terms*—Conceptual design, integrated design, mechatronics, model reduction, robust control.**

I. Introduction

MECHATRONICS is the science of motion control [1]. A mechatronic system consists of a mechanical structure where actuators generate the required motions, where sensors measure the resulting motion, and where a control algorithm cancels out the differences between the resulting motion and the desired motion specified by the task programming system.

Designing mechatronic systems entails the design of an optimal mechanical structure and of optimal motion control systems. The problem is that both the mechanical and the control behavior interact with each other. This means that the traditional sequential engineering approach can never lead to optimal system behavior. Indeed, a classical design rule-of-thumb is that the motion control system bandwidth should be less than half the lowest natural frequency of the controlled mechanical structure in order not to excite these frequencies. There is a need for a concurrent engineering approach, where mechanical and control behaviors are simultaneously optimized. Such an approach allows one to extend dramatically the control bandwidth, eventually far beyond the lowest natural frequency. This calls for a so-called mechatronic compiler, where high-level design specifications are (semi)-automatically translated into an optimal mechatronic system and whereby the mechanical structure and motion controller are considered to belong to one single system to be optimized.

In this paper, some approaches are presented that may ultimately lead to a fully fledged mechatronic compiler. First, an optimizing preliminary design approach is presented for a limited category of mechatronic systems, namely, machine tools with three perpendicular axes. The result is an optimized design in the conceptual state, ready for detailed (simultaneous) design.

In the second part, an approach is proposed, based on component mode synthesis, for synthesizing full state-space control models of mechatronic systems with variable configuration, obtained by combining finite-element models of the constituting mechanical and drive components.

In the third part, a robust controller synthesis method is presented that leads to optimal motion behavior of the machine in its different configurations, thereby fully taking into account the (changing) system dynamics.

II. Conceptual Design of Three-Axis Machine Tools

This section presents an approach for the synthesis, analysis, and optimization of the conceptual mechanical structure of three-axis machine tools. The machine tool configurations are described by ten *configurational parameters* by which the different machine variants are configured. The variants are assembled from a parametric component library. These components have parametric shapes and dimensions (the *geometric parameters*). Three analyses are developed for the evaluation of the generated machine variants: 1) a *static analysis*, calculating the static stiffness; 2) a *dynamic analysis*, calculating the natural frequencies; and 3) a *clearance analysis*, checking the geometric interference between the components. The optimizations of the configurational and of the geometrical parameters are carried out by *genetic algorithms*. The optimization objectives can be to maximize the static stiffness, and/or to maximize the lowest natural frequency, and/or to minimize the geometric interferences. The results of this conceptual design can be used for further, more detailed, mechatronic design of the structure and of the controller.

A. Description and Model of Three-Axis Machine Tools

The conceptual model of the generic three-axis machine tool structure under study is represented in Fig. 1. This model and its description system are adopted from Lipóth [2]. The generic machine structure is described as an open chain of *four members*: the headstock (HST) with the main spindle, the member next to the headstock (NT_HST), the member next to the table (NT_TBL), and the table (TBL). The member at one end of the chain is the HST, and the one at the other end is the TBL. One of the four members is *fixed* to the ground. The fixed member is always constructed from two parts; therefore, one machine is constructed from *five components*. (In the figures, dots indicate the two components of the fixed member.) The four members are connected by *three linear guideways:* the headstock guideway (*HST_GW*) connects the HST and the NT_HST; the middle guideway (*MID_GW*) connects the NT_HST and the NT_TBL; and the table guideway (*TBL_GW*)

Manuscript receivedSeptember 24, 1999; revised March 15, 2000. This work was supported by the Soros Foundation, Flemish Foundation for Scientific Research, EU (BRITE/EURAM), and Belgian Programme on Interuniversity Poles of Attraction initiated by the Belgian State, Prime Minister's Office, Science Policy Programming. Recommended by Technical Editor B. Ravani.

The authors are with the Katholieke Universiteit Leuven—P.M.A., Leuven, Belgium.

Publisher Item Identifier S 1083-4435(01)02727-2.

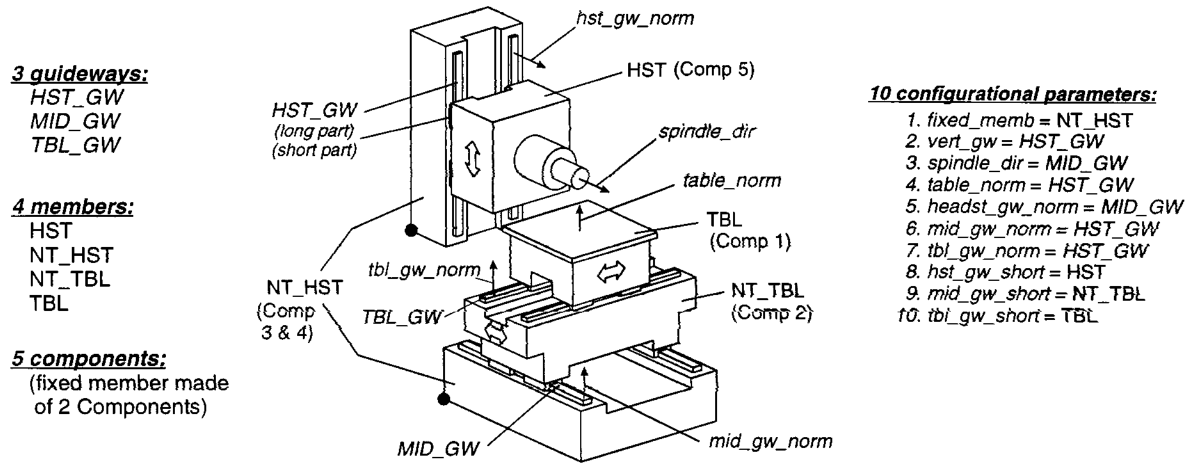

Fig. 1. Conceptual model of a three-axis machine tool with orthogonal axes.

connects the NT_TBL and the TBL. The directions of the three guideways are perpendicular to each other, and one of them is vertical. The guideways have a *long part* and a *short part* connecting two adjacent members/components. The direction of the spindle, the direction of the table normal, and the directions of the three guideway normals are parallel with the direction of one of the guideways.

From this description system, ten configurational parameters can be defined, which determine all the possible configurations of three-axis machine tools. They, and the possible values they can take (values in curly parentheses), are as follows:

fixed_memb: which member is fixed to the ground {HST, NT_HST, NT_TBL, TBL};
vert_ gw: which guideway is the vertical guideway {*HST_GW, MID_GW, TBL_GW*};
spindle_dir: direction of the spindle axis {*HST_GW, MID_GW, TBL_GW*};
table_norm: direction of the normal of the table plane {*HST_GW, MID_GW, TBL_GW*};
hst_gw_norm: direction of the normal of the *HST_GW* plane {*MID_GW, TBL_GW*};
mid_gw_norm: direction of the normal of the *MID_GW* plane {*HST_GW, TBL_GW*};
tbl_gw_norm: direction of the normal of the *TBL_GW* plane {*HST_GW, MID_GW*};
hst_gw_short: which member has the short part at the *HST_GW* {HST, NT_HST};
mid_gw_short: which member has the short part at the *MID_GW* {NT_HST, NT_TBL};
tbl_gw_short: which member has the short part at the *TBL_GW* {NT_TBL, TBL}.

The ten configurational parameters are independent from each other, and any combination of them can describe a unique machine tool configuration. The total number of all possible machine variants is 6912, obtained by multiplying the numbers of the possible values of the ten parameters ($4 \cdot 3 \cdot 3 \cdot 3 \cdot 2 \cdot 2 \cdot 2 \cdot 2 \cdot 2 \cdot 2 = 6912$). These 6912 variants are called *main variants* because several subvariants can be configured for each combination of the ten configurational parameters. Clearly, five of the ten parameters, namely, *spindle_dir, table_norm, hst_gw_norm, mid_gw_norm,* and *tbl_gw_norm* describe orientations without senses. But, depending on the combinations of the ten parameters, most of these five directions can have two senses. For instance, if we take a look at Fig. 2, we can see an example of the alteration on the direction of the *table_norm, tbl_gw_norm,* and of *mid_gw_norm* for a particular machine configuration.

The total number of possible subvariants of this main variant in Fig. 2 is eight. This kind of alteration of directions leads to the creation of numerous subvariants. Some main variants have only two subvariants (e.g., see the machine of Fig. 1), and some of them have 16 subvariants. An exact mathematical deduction of the number of possible subvariants is not available. But, using special rules and algorithms, these subvariants can be derived and configured from each main variant, and the total number of them can be counted, by the use of a computer program, if we go through all the possible 6912 main variants. The total number of possible subvariants is 56832. These subvariants are unique configurations (each of them is different). From the configurational point of view, they are of equal rank (none of them is superior), and they constitute the complete design space of the three-axis machine tools under study.

B. Configuration of the Machine Variants

1) Model of the Guideways: The linear guideways in the description system have a long part and a short part that move relative to each other. In the design system, we apply the frequently used concept where the long part is constructed from two rails, and the short part is constructed from four carriages. The conception of the mechanical model of the machines (see Section II-C1) is also based on this four-carriages-two-rails guideway concept.

2) Parametric Component Library: The machine variants are configured from a component library where each component has parametric shapes and dimensions. The components and their assemblies are modeled in a state-of-the-art computer-aided design (CAD) system using parametric multipart solid modelling. The components are classified in an object-oriented way, and their assembly and data manipulation

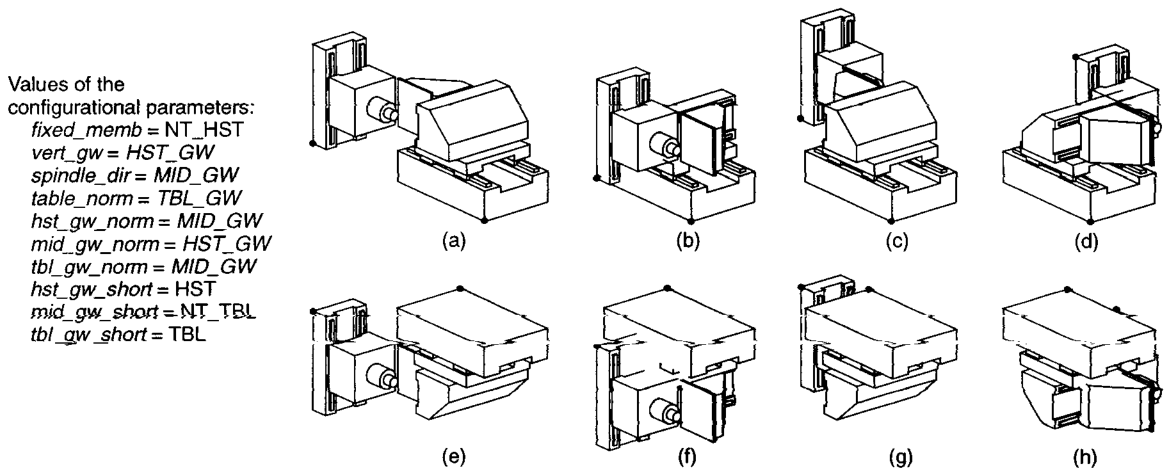

Fig. 2. Example for generation of subvariants of a particular main variant.

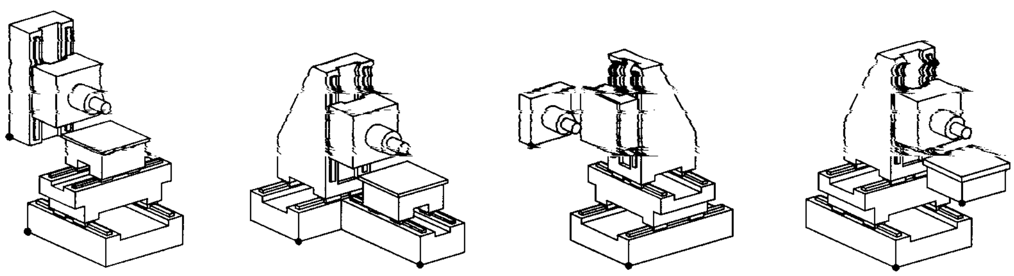

Fig. 3. Examples of the four major classes of three-axis machine tool configurations.

are programmed using object-oriented programming. We can distinguish four major component classes: the Fixed Guide, the Headstock, the Table, and the Slide. For example, each machine of Fig. 2 is configured from two Fixed Guides, a Headstock, a Table, and a Slide. Several other classifications have been made so that every machine tool variant can be configured utilizing the advantages of abstraction and polymorphism of object-oriented design and programming. For instance, an abstract class Moving Component is defined for the components that can move on a guideway and another abstract class Carrier Component is defined for components on which other component can move. Currently, there are 52 components in the library: two Fixed Guides, 11 Headstocks, 11 Tables, and 28 Slides.

3) Configuration of the Different Machine Classes: The machine tools are grouped in four major classes depending on which member is the fixed member. These four classes can be seen in Fig. 3. Each machine tool class has special selection tables that define the components to be used for configuring the machine of that kind. These selection tables are functions of the configurational parameters. During configuration time, the geometric parameters of the components are set and linked with parameter expressions. The strokes of the linear guideways and the order of magnitude of the main dimensions of the components are derived from the workspace dimensions (input). After configuring the machines, the values and/or the expressions of the geometric parameters can be modified by the user (manually) or by the optimization algorithms (automatically; see Section II-D). Fig. 4 demonstrates some examples obtained by modifying the geometric parameters of the machine tool of Fig. 1.

4) Constraining the Design Space: The entire design space, 6912 main variants and 56 832 subvariants mentioned above, is extremely huge. Therefore, several constraints have been set in order to restrict/filter the design variants of interest. Some of these constarints are the following.

1) Enable horizontal or/and vertical spindle.
2) Enable horizontal or/and vertical table (e.g., machines in Fig. 2 have vertical table plain).
3) Enable symmetric or/and asymmetric machines. The plane of symmetry is determined by the parameters *spindle_dir, table_norm, hst_gw_norm, mid_gw_norm* and *tbl_gw_norm*. The machine is symmetric if these five direction vectors are coplanar.
4) Enable mirrored machines or not. In case of asymmetric machines, there are always one or more subvariant pairs where two machines are mirrored versions of each other. The rules to decide these cases are too complex to present in this paper, but for demonstration, in Fig. 3 there are four pairs of mirrored machines: 3a is the mirrored version of 3c, 3b is of 3d, 3e is of 3g, and 3f is of 3h.

Some of these constraints can be evaluated directly from the ten configurational parameters, but in several cases the direction vectors of the components being configured must be examined. The configuration algorithms are developed in a way such that a quick checking of constraint violations can be possible (it was

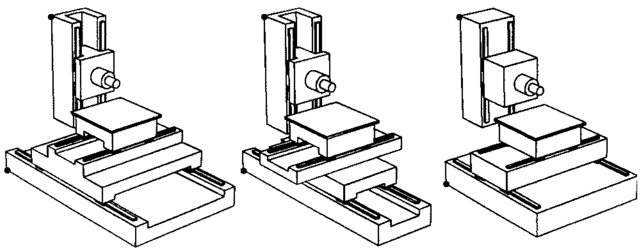

Fig. 4. Modifications of the geometric parameters.

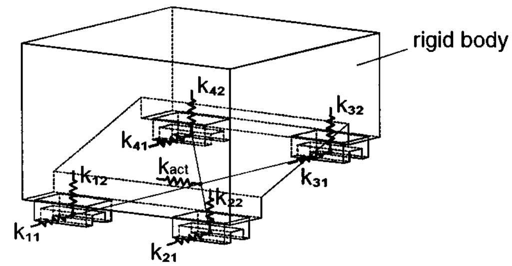

Fig. 5. Mechanical model of the guideways.

necessary because the configuration time of one machine takes 20–25 s on an HP 9000/782/C200+ workstation, so that the configuration of all the 56832 machine would take 13–14 days). In these cases, the special direction vectors and transformation matrices of the components are loaded without loading of their CAD model. Then the checking of constraint violations and the counting of machine variants are done, but the configuration of the real components do not take place. Thus, an examination of the entire design space (56 832 machines) can be realized in a very short time (in some seconds). Here, some subsets of the design space can be seen that are obtained by different constraint settings.

1) There are 1536 symmetric main variants that have 8960 subvariants.
2) There are 5376 asymmetric main variants that have 47 872 subvariants that are 23 936 $(47\,872/2)$ mirrored pairs.
3) There are 384 asymmetric main variants that have a vertical spindle and a horizontal table plane facing upwards, and these main variants have 640 not-mirrored subvariants.

C. Analyses of the Generated Machine Variants

There are three types of analysis developed to evaluate the generated machine tool variants: static, dynamic, and clearance.

1) Mechanical Model: For the static and dynamic analysis, the guideways and the transmission elements are represented by linear springs and the bodies of the components are assumed to be rigid. Fig. 5 shows the mechanical model of the guideways. Every carriage is modeled by two linear springs in its center point. The actuator (e.g., lead screw) is also modeled by a spring (k_{act}) and is placed in the center point of the other eight springs. The three guideways of the machine tools are modeled in the same way, resulting in 27 springs in the entire mechanical model.

2) Static Deformation Analysis: For calculating the static deformations, homogeneous transformations, stiffness matrices, force moment transformations, and matrix algebra are used, applying the mechanical model presented above. The matrices are constructed using the parametric geometrical data of the assembled components. The relative displacements between the table (workpiece) and the spindle are calculated for some discrete spindle positions along the motion range, applying a particular cutting force as a static load at the end of the spindle. This method provides a fast numerical computation to estimate the static stiffness of the generated machine tool variants. Fig. 6 shows an example of static deformation analysis for the case of a machine tool where the fixed member is the neighbor of the table. The calculations are made for three positions of each Moving Component. Since the three Moving Components have three positions on each guideway, there are $3^3 = 27$ discrete spindle positions. These positions are indicated on the horizontal axis of Fig. 6. The first digit denotes the position of the component on the *HST_GW,* the second digit indicates the position of the component on the *MID_GW,* and the third digit denotes the position of the component on the *TBL_GW*. A "0" means that the component is in the starting position (position closest to the origin of the coordinate frame); "1" means that it is in the middle; and "2" means that it is at the other end. The curves in Fig. 6 indicate the Euclidean norms of the rotational and translational displacement vectors.

3) Dynamic Analysis: ROBOTRAN [3] is used for generating the symbolic dynamic equations to calculate the natural frequencies of the machine tool structures. It is a software tool specially developed for multibody system analysis. ROBOTRAN computes the multibody equations of motion using the Newton/Euler recursive scheme with explicit and recursive extraction of the mass matrix of the system. It generates symbolic equations of motion in a very compact form. This means that data (such as some vector or inertia components) being equal to "zero" for the envisaged application are eliminated from the dynamic expressions. This allows to avoid the unnecessary operations ("$0 + A$," "$0 \cdot A$," "$1 \cdot A$"), and consequently to save CPU time during the numeric application of the symbolic equations [3].

The symbolic dynamic equations of the four main basic classes of the machine tools under study have been generated by ROBOTRAN, beforehand, and these can be used during the numerical analysis or optimization of the synthesized machine tools. The mechanical model shown above (Fig. 5) is applied to model the machine tools as multibody systems. Each guideway is modeled in a way that three-dimensional motion can be allowed between the adjacent components (in essence, it is a six degree-of-freedom joint). Each component is linked by nine linear springs and dampers. Therefore, each machine tool has $3 \cdot 6 = 18$ degrees of freedom for the dynamic analysis. A numerical program has been developed to calculate the natural frequencies of the synthesized machine structures. This program numerically solves the symbolic dynamic equations generated by ROBOTRAN. The input (geometry, masses, inertia tensors, etc.) for this numerical process is extracted from the CAD system in which the machine tool models

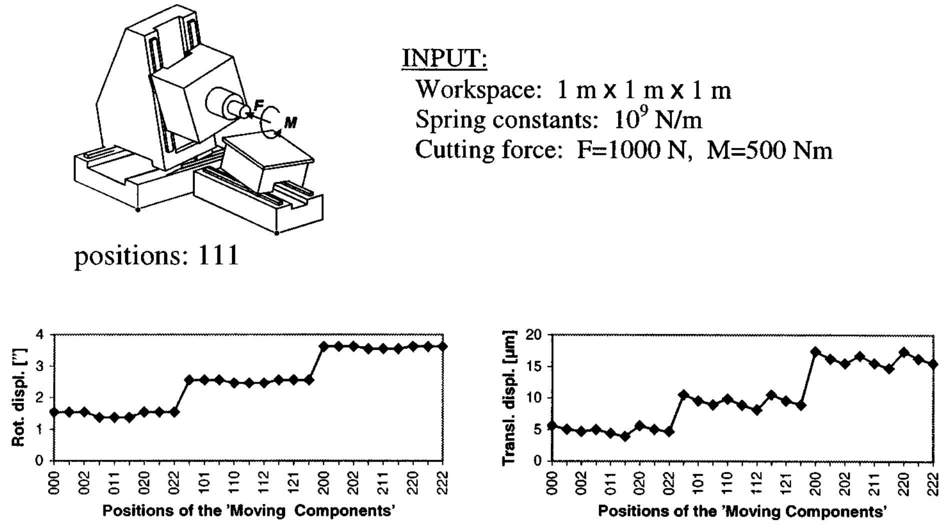

Fig. 6. Example of static deformation analysis.

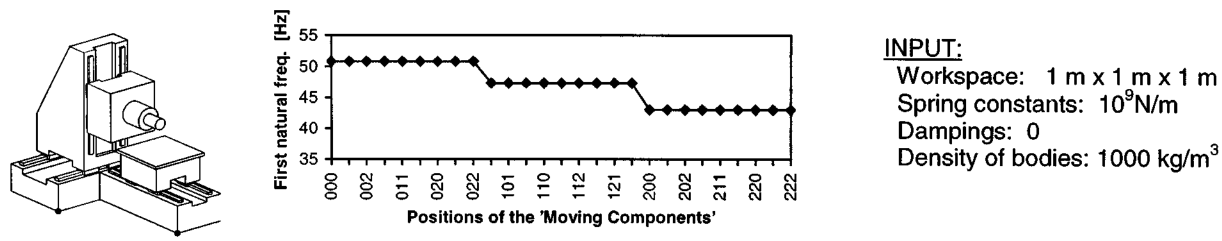

Fig. 7. Natural frequencies of a particular machine tool.

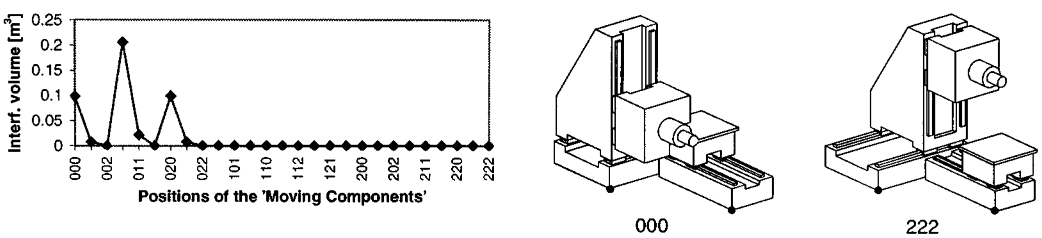

Fig. 8. Total volume of the interference objects of a three-axis machine tool.

are constructed. Fig. 7 demonstrates an example for the first natural frequencies of the same machine tool and of the same 27 positions used in Fig. 6.

4) Clearance Analysis: Since the components can move on their guideways, they can possibly interfere with each other, or, in case of improper design, they can steadily interfere. During clearance analysis, the interference between the components of the assembly is checked and calculated for any position of the spindle in the workspace. The aggregate volume of the interference objects has been chosen as a measure of the interference belonging to one spindle position of a particular machine tool. These aggregates are calculated for different (discrete) spindle positions. The cumulated sum of these aggregates divided by the total volume of the machine serves as a measure to estimate the clearance of the machine tools. From the clearance analysis point of view, the "better" the machine tool the lower this value. The clearance analysis can be programmed and carried out in the CAD system in which the design system is realized. In Fig. 8 the total volume of the interference objects is depicted for the same machine tool of Figs. 6 and 7, and for the same Moving Component positions. On the right side of Fig. 8, two situations are shown: 000 is the situation where the three Moving Components are in their starting positions; and 222 is the case where these components are at the other end of the guideways.

D. Optimization of the Generated Machine Variants

The analyses presented above can be used as a valuable tool to assess and compare different configuration variants. They can also serve as objective functions for optimization.

1) Optimization with Genetic Algorithms: Genetic algorithms (GAs) are applied to search for optimal parameters of the three-axis machine tools represented and modeled above. GAs differ from traditional optimization techniques in four fundamental ways [4].

1) They work using an encoding of the parameters to be optimized or searched for, not the parameters themselves.
2) They search from one population of solutions to another, rather than from individual to individual.
3) They use objective function information, not an auxiliary information or derivatives.
4) They use probabilistic, not deterministic, transition rules.

The first step in solving a problem using GAs is to develop a method of encoding the parameters into the so-called chromosomes. At the beginning of genetic search, a population of individuals is initialized by randomly selecting members from the allowable space on the method of parameter encoding used. Then, each member of the population is evaluated. Next, an iterative loop is entered in which some members of the population are selected for the next generation. These members are recombined to form the population of the next generation, and finally the members of the new generation are evaluated. From generation to generation the average value, the so-called fitness value, of the individuals evolves and converges to a global optimum. This process imitates the evolution observed in nature.

The optimal values of the ten configurational parameters and/or the optimal values of the geometrical parameters of the components can be searched for. GAs provide a robust method for these optimizations, which means that the optimization criteria and the number of the parameters to be optimized can be easily modified. The optimization criteria can consist of one or more from the following objectives: 1) to maximize the static stiffness; 2) to maximize the lowest natural frequency; and 3) to minimize the geometric interference. The user of the system can choose from these objectives and combine them. The objective functions, and indirectly the fitness values of the individuals, for GAs are composed by summing the weighted values resulting from the chosen analyses.

GAs perform reasonably well as a search method for optimization. The so-called steady-state genetic algorithms, which use overlapping populations [4], have been applied because the calculation of the objective functions takes a considerably long time (e.g., the average time of the static analysis and of the clearance analysis for 27 spindle positions is about 40 s on an HP 9000/782/C200+ workstation; the calculation of the dynamic analysis for 27 spindle positions takes about 3 min on the same workstation). Because of the parallel nature of GAs, the optimization time can be significantly reduced by parallel processing. Therefore, parallel GAs have been developed where each individual of a GA population can be evaluated on different workstations in parallel.

2) Optimization Case Study: The machine configuration and the analysis inputs under this case study are the same as in Figs. 6–8. The optimization criterion is to find the optimal values of two geometrical parameters—the height of the headstock and the height of the table—in view of minimizing the static deformations and the geometric interferences and maximizing the first natural frequency. The range of both of these two geometrical parameters is 200–700 mm.

At the top of Fig. 9, the analysis results can be seen. The first chart (top left) and the second chart (top right) of Fig. 9 depict the results of the static analysis. The values of these two charts are obtained by summing the aggregate values of the rotational and translational displacements (see Fig. 6) for the cases of different headstock and table heights. The third (middle left) chart of Fig. 9 shows the results of dynamic analysis. The values are the first natural frequencies when the three moving components of the machine tool are in the middle. The fourth chart (middle right) depicts the results of the clearance analysis (see Section II–C4). Using a weighting method, these four measures are added, resulting in a fitness function that is applied for optimization by genetic algorithms. This fitness function for GA is presented at the bottom of Fig. 9. It can be seen that there is an optimal combination of the headstock and table height, coinciding with the peak of the surface. GAs are able to find it even when local optima are present. Fig. 10 demonstrates the physical meaning of the optimal values of the headstock height (h) and of the table height (t). From the static and dynamic analysis point of view, the better the machine, the lower these values (see bottom and right of Fig. 10). From the clearance analysis point of view, the better the machine, the higher these values (see top and left of Fig. 10). The optimum can be found somewhere in the middle of the range of the parameters.

Fig. 11 shows the results of two optimization examples of these two geometrical parameters using GA. At the first examples (see left side of Fig. 11), the resolution of the two parameters to be optimized was set to 50 mm, and at the second one (see right side) was set to 10 mm. At the top of the picture the GA parameters can be seen (they were the same for both runs).

Successful optimizations have been done for more than two parameters. The application of GAs for these kind of optimisation problems has several advantages.

1) Chromosomes can easily be concatenated for a variable number of parameters to be optimized.
2) There is no need for analytical or numerical derivation of the objective functions.
3) Global optima (or more sub-optima in parallel) can be found.

The main disadvantage is long computation time, which is less and less a problem nowadays with the availability of fast workstations and the possibilities of parallel computation techniques.

E. Conclusions for Conceptual Design

The system presented in this section exhibits a novel approach to the conceptual design (synthesis, analysis, and optimization) of three-axis machine tool structures. It is also a good demonstration of the integration of a state-of-the-art CAD tool (Unigraphics CAD/CAM/CAE system), Matlab as a computational engine for dynamic analysis, a multibody dynamics tool (ROBOTRAN), and artificial intelligence tools (genetic algorithms, and object-oriented design and programming using C++).

This conceptual design framework is a valuable tool to assist the designer in exploring the entire design space. This may lead

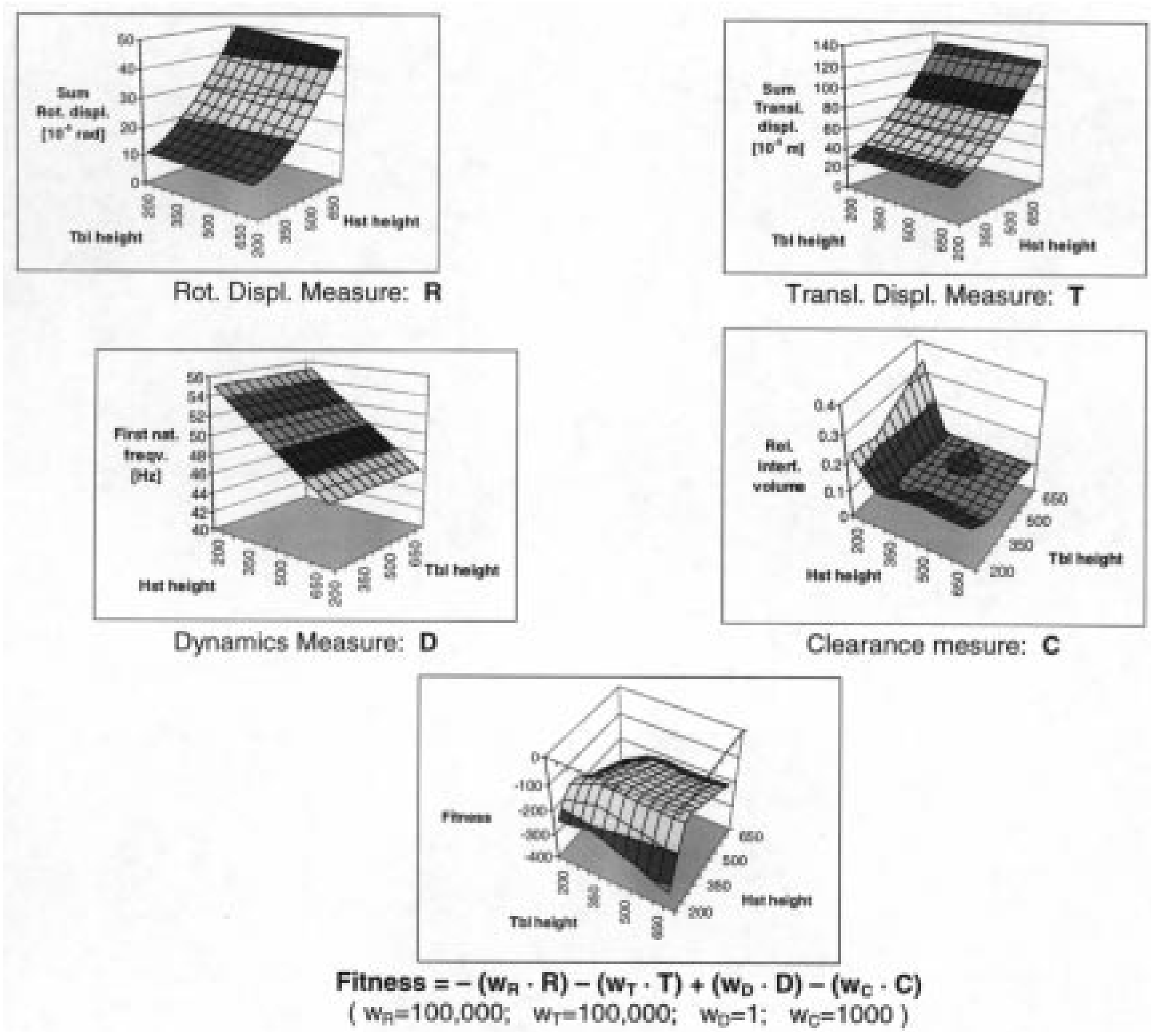

Fig. 9. Derivation of fitness function for static and clearance analysis.

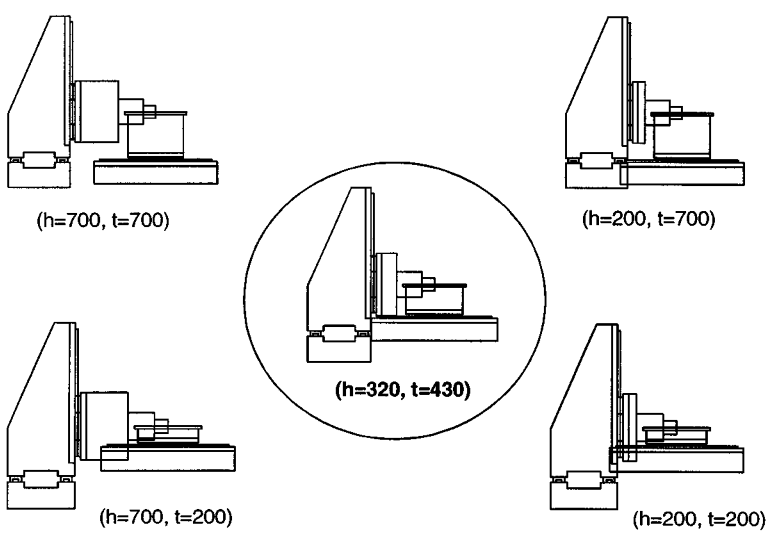

Fig. 10. Optimal values of the headstock height (h) and of the table height (t).

to feasible design configurations that would never have been conceived by an "intuitive" designer.

The resulting "optimal" conceptual design is an excellent starting point for further, more detailed mechatronic design of

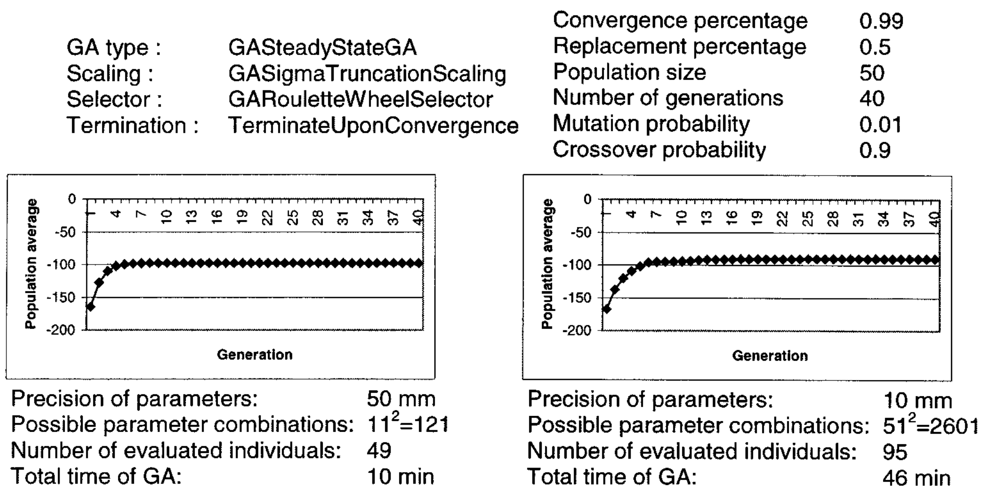

Fig. 11. Example for optimization of two geometric parameters using GA.

the structure and of the motion control system. The first step in this procedure is the detailed design of the different individual components. This requires specialized design expertise, available in the heads of experienced designers, and, more and more, in design databases and expert systems. The result of this step is a set of finite-element models of the machine components. This design step is not described in this paper. The component models are assumed to be available. What will be described in the sequel is their use for composing dynamical models of the complete machine tool and the use of these composite models for designing robust motion control systems.

III. Dynamic Model Reduction of a Flexible Three-Axis Milling Machine

A. Introduction

An adequate description of the dynamic behavior of a complex mechanical structure is based on a finite-element model, usually with a very large number of degrees of freedom. The reduction of this finite-element model into a model of much smaller dimensions, suitable for control system design, forms a necessary step in the development of a mechatronic compiler.

An important class of mechatronic systems, like machine tools and robots, has a large number of different operational positions. Their dynamic behavior, described by their eigenfrequencies and mode shapes, will change with changing working configuration. This will inevitably affect the performance and the robust stability of the control system, and should therefore be taken into account during controller design.

This section focuses on the design of a three-axis high-speed milling machine for the superfinishing of dies and molds, as a representative example of a complex mechatronic system. As the milling operation is very time consuming, a faster machine that works at higher speeds while keeping the required accuracy would yield a significant reduction in production costs.

This paper shows that the component mode synthesis (CMS) technique [6] provides an appropriate solution for the dynamic analysis of the machine in different working configurations and for the conversion of the machine model into a reduced model for control system design. Moreover, the method developed in this study accurately simulates the tracking behavior of the flexible machine in its entire working domain, because the machine model can be cheaply assembled in any desired position.

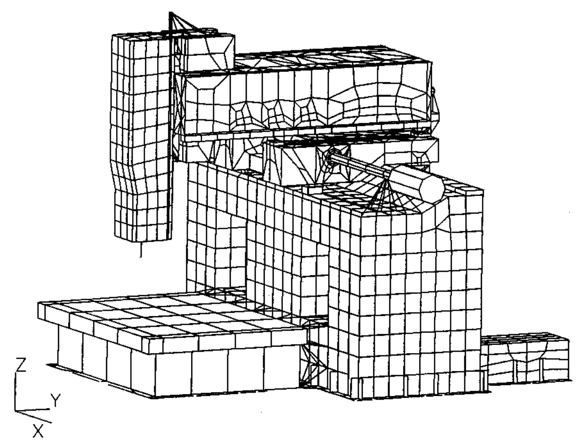

Fig. 12. Finite-element model of the machine tool.

The machine analyzed here is represented by its finite-element model in Fig. 12. This model has 30 598 degrees of freedom.

B. Elaboration of the Proposed Reduction Method

The discussion in this section focuses on the three-axis milling machine, but the methodology can be readily applied to other (flexible) multibody structures. The proposed reduction method makes use of two standard engineering software packages. All finite-element calculations are performed within MSC/Nastran. The Matlab environment is used to coordinate the assembly of the machine in the desired spatial configuration; to convert the modal machine model, obtained from MSC/Nastran, into a state-space model; and to perform the subsequent control system synthesis and analysis.

Fig. 13 shows the different steps in the method; they are extensively discussed in [7].

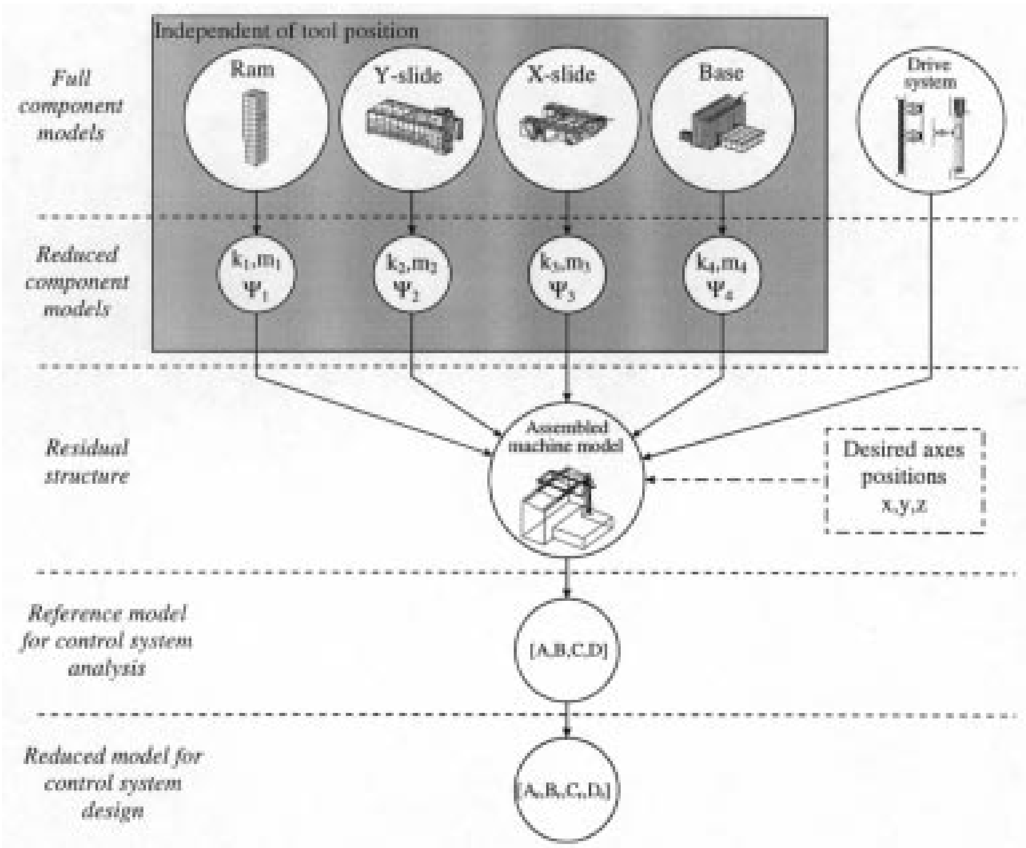

Fig. 13. Overview of the proposed reduction method.

1) First Component Mode Reduction and Synthesis Step: The construction of the three-axis milling machine allows a natural definition of the components as the ram (machine Z-axis), the Y-axis slide, the X-axis slide, and the base. These components are represented in Fig. 13 by their finite-element models in the upper part of the gray box. The modal models of the four components of the milling machine are obtained from a standard component mode reduction and are stored on hard disk as four separate MSC/Nastran databases. They are represented in the lower part of the gray box in Fig. 13 by their respective component modal stiffness and mass matrices, k_i and m_i, and by their component mode vectors Ψ_i.

The residual structure, on the third level in Fig. 13, is the finite-element machine model after numerical condensation of the components. In the assembly phase, the reduced component models are attached to the residual structure as "external superelements," each defined in a different relative coordinate system. These relative coordinate systems allow the assembly of the components in the appropriate relative positions. The locations of these relative coordinate systems, which actually determine the location of the tool tip in the operation space of the milling machine, are defined from within Matlab.

The component modal models should be independent of the spatial configuration of the milling machine, and may, therefore, not contain any element of the drive chains. These drive chains for the three slides, represented on the right of the gray box, belong to the residual structure as their dynamic properties depend on the relative positions of the two slides to which they are connected. For example, when considering a ballscrew drive, the dynamics of the drive depend on the position of the nut on the screw.

TABLE I
DIVISION OF THE DEGREES OF FREEDOM IN INTERIOR AND EXTERIOR DEGREES OF FREEDOM FOR THE FOUR COMPONENTS

	ram	Y-axis slide	X-axis slide	base
interior dofs	1714	3496	3436	19738
exterior dofs	324	408	138	462
total number of dofs	2038	3904	3574	20200

Several sets of modes can be used to form the component models. The choice of these sets has a great impact on the accuracy of the reduced model. The time required to perform an analysis of the machine in one configuration is mainly determined by the number of modes that are taken up in the component modal models. This number of modes is strongly influenced by the number of external degrees of freedom of the components, because MSC/Nastran always takes up all constraint modes (which are identical to the Guyan reduction vectors) in the modal base of a component. The numbers of internal and external degrees of freedom of each component are shown in Table I. The entire model has 30 598 nodal degrees of freedom, of which 882 belong to the residual structure (the guideways and the drive chains) and are therefore not mentioned in Table I.

In the classical Craig–Bampton method, the constraint modes are supplemented with some fixed-interface normal modes of

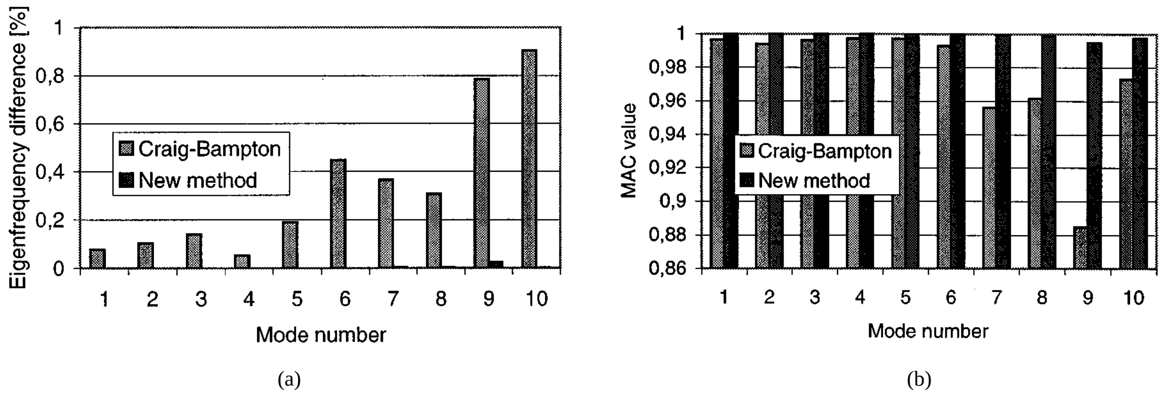

Fig. 14. Accuracy of the Craig–Bampton and the new CMS method in comparison with the full model. (a) Relative eigenfrequency difference and (b) MAC-value of the mode shapes.

vibration [6]. However, much more accurate results are obtained by a new alternative method that combines the constraint modes with a few free-interface normal modes and the set of six inertia-relief modes. The left-hand part of Fig. 14 shows the relative eigenfrequency differences between the lowest ten modes, calculated with the CMS method and with the full model with 30 598 degrees of freedom. The right-hand part of Fig. 14 shows the spatial correlation, as given by the modal assurance criterion (MAC [8]), between the lowest ten eigenmodes calculated with the CMS method and the corresponding modes calculated with the full model. The results presented in Fig. 14 indicate that the correlation between the actual mode shapes of the full model and those calculated with this new component mode synthesis method is almost perfect. Moreover, the relative eigenfrequency difference has been reduced by a factor of 30 compared to the Craig-Bampton method. The reason for this nearly perfect correlation is the fact that the inertia-relief modes account for the residual effects of the omitted high-frequency normal modes at zero frequency, yielding an exact representation of the static deformation of the component, loaded by the inertial forces due to a uniform acceleration. Analogously, the static deformation due to concentrated forces in the exterior nodes is exactly represented by the constraint modes [9].

The assembled residual structure of the machine, as depicted in Fig. 13, is obtained from MSC/Nastran by defining dedicated “plot elements” between the external nodes of the four components and a few extra nodes on the base (coincident with the actual corner nodes of the base, but without any physical meaning).

2) Second Component Mode Reduction Step: This assembled residual structure is then further considered in the second reduction step as a single component. It has only nine external degrees of freedom, being, on the one hand, the rotations around the three motor axes, on which the torque input for generating the desired trajectory is applied, and, on the other hand, the six degrees of freedom of the tool, on which possible external disturbance forces, originating from the cutting process or from a spindle unbalance, apply. The component mode reduction projects the degrees of freedom of the residual structure on a modal base consisting of nine constraint modes, 36 fixed-interface normal modes, and six inertia-relief modes. The number and type of component modes in this modal base have again been selected such that the correlation with the original full model is almost perfect in the frequency band of interest [7]. This second component mode reduction is performed with a dedicated MSC/Nastran DMAP-alter [10] that writes the reduced mass, stiffness, and damping matrix and the modal transformation matrices to an ASCII file. These matrices are then converted into a state-space model in Matlab. This state-space model, represented by the matrices $[A, B, C, D]$ in Fig. 13, forms a reference model for the design of a control system for the motors of the machine axes. A major part of this second reduction step is based on the work reported in [11].

The order of the reference model $[A, B, C, D]$ is still considerably high. In the case of the milling machine, this reference model is obtained from a component modal model with about 50 modal degrees of freedom, resulting in a state space representation with about 100 states. Prior to the control system synthesis, this reference model is again reduced to a state-space model of much lower order, represented by $[A_r, B_r, C_r, D_r]$ in Fig. 13. Different methods, including, for example, the balanced truncation method or the Hankel norm approximation method, are available for performing this third reduction step. This third reduction step is typically related to the control system design. Both this model reduction and the controller design are treated in Section IV of this paper.

C. *Conclusions for Model Reduction*

This section proposes a dynamic model reduction scheme that enables an accurate and computationally efficient study of the dynamic characteristics of flexible mechatronic systems in multiple spatial configurations. Such a dynamic analysis module forms an essential part of a virtual prototyping environment for mechatronic systems.

The proposed reduction scheme essentially consists of a multistage component modal reduction and synthesis procedure. In each step, the accuracy of the reduced model can be well preserved relative to the full original finite-element model, by a judicious selection of the type and number of component modes in the modal transformation matrix. It appears in this study that inertia-relief modes are always beneficial in that sense.

Also, the partition of the full finite-element model into individual components plays an important role in the proposed

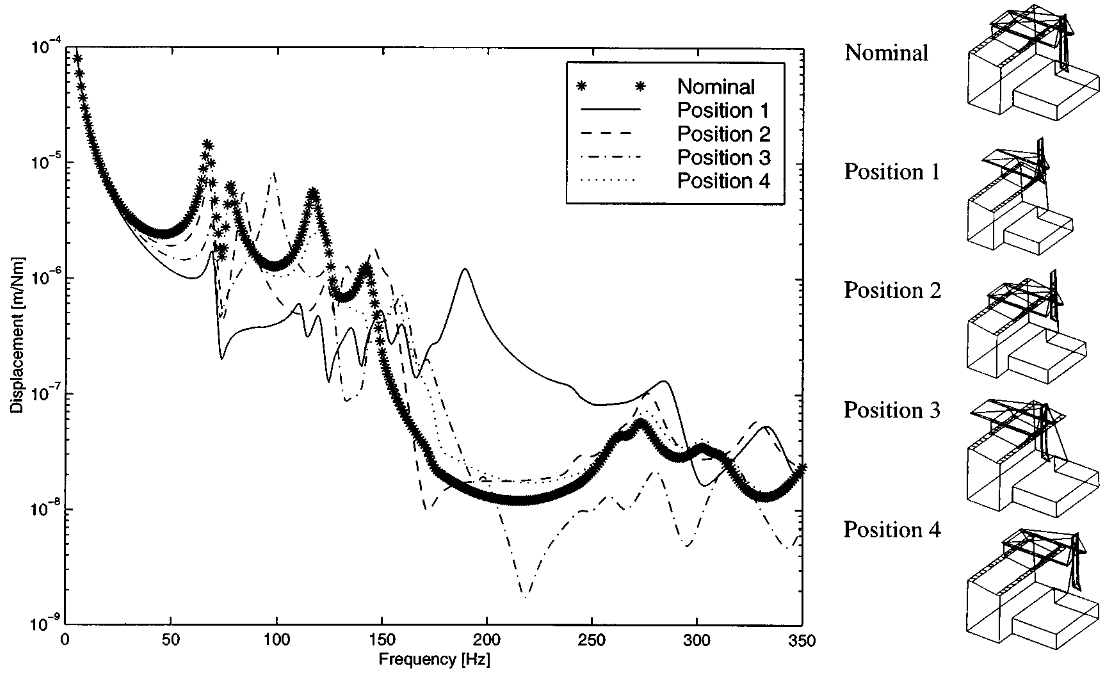

Fig. 15. Transfer function from the X-axis motor torque to the X-displacement of the tool for five different spatial configurations of the machine tool.

method. A definition of the components independently from their relative positions allows a quick dynamic analysis of the machine in different spatial configurations, or an accurate evaluation of the tracking behavior of the machine over a large trajectory. The influence of the changing tool position on the dynamic behavior of the machine tool is illustrated in Fig. 15 that shows the same transfer function from X-axis motor torque to X-displacement of the tool for five different tool positions.

The next step presented in this paper is the development of a tracking control system for the three machine axes. This control system should be robust against the inevitable model inaccuracy. One important type of model inaccuracy is due to the changing machine configuration, which varies with the desired working position of the tool. The analysis of the machine dynamics in different configurations allows us to derive a more accurate estimate of the machine model uncertainty used for control system design.

IV. Robust High-Bandwidth Motion Control

A. Introduction

The ever-growing competition on the international markets pushes manufacturers towards shorter design cycles and decreasing manufacturing times for their products. This reduced time-to-market pressure generates a demand for faster machine tools that can reduce machining time, while preserving or improving the final accuracy. Machine tool producers try to meet these goals by designing light, but rigid, mechanical structures. With the existing materials, it is presently very difficult to further reduce the weight in an economic way without reducing the stiffness. This makes it difficult to achieve more acceleration, without losing accuracy. The requirement of higher speeds and accelerations makes this problem even more complicated, since this will result in trajectories with higher frequency content, and higher closed-loop bandwidths, which in turn will excite more the structural vibrations.

State feedback algorithms allow us to take flexible modes into account in the control model, thereby changing the dynamic behavior of these modes. This can be used to add damping to the modes, or to increase the resonance frequency. Including more modes in the control model allows controlling more modes, but it also increases the controller complexity. Similar approaches to robot flexibility control [12], [13] consider that the first eigenfrequency dominates the structural dynamics, and consequently higher order dynamics could be neglected. This can be assumed for a robot arm, but not for more complicated flexible structures, such as a machine tool. In a machine tool, the structural vibrations are determined by a relatively large number of modes, which usually lie very close to each other, as is clear from Fig. 15.

For mechatronic systems with variable configuration, like the machine tools discussed in this paper, the need arises for robust controllers that guarantee robust performance over the entire configuration space. Good examples of robust controllers are H_∞-controllers and sliding-mode controllers.

The discussion on flexibility control will be limited to the X-direction. The machine tool flexibility in X-direction is determined by the flexibility of the X-axis drive chain and by the structural flexibility of the slides of the Y- and Z-axes of the machine. In order to control the flexible modes of the X-axis, a position sensor, integrated in one of the slideway carriages of the X-axis, essentially measures the vibrations induced by the X-axis drive chain flexibility, while an accelerometer, mounted near the tool, observes the vibrations due to the structural flexibility of the machine Y- and Z-axes.

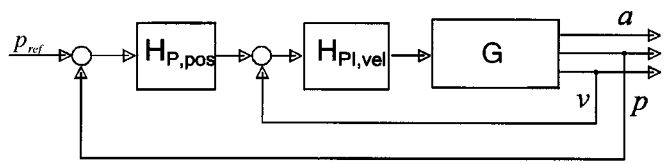

Fig. 16. Reference PID controller (p_{ref}: reference position; p: actual position; v: actual velocity; a: actual acceleration).

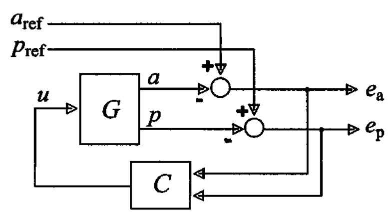

Fig. 17. The H_∞ controller scheme.

B. The Reference PID Controller

The controller parameters have been determined by an iterative procedure on a simulated system [11]. They have been selected so as to minimize the settling time without introducing overshoot in the step response measured at the X-axis sensor. The reference proportional/integral/derivative (PID) controller contains an internal velocity feedback loop enclosed by a proportional position feedback loop, as shown in Fig, 16. There is no tool acceleration feedback, but tool acceleration is monitored to allow comparison with the controllers developed below.

C. The H_∞ Controller

A PID controller only feeds back the motor velocity and the axis position. Its simple structure allows an easy design and implementation. However, the limited amount of controller parameters allow us only to control the rigid body mode directly. Hereunder, the development of an H_∞-controller for the three-axis milling machine discussed above is presented. The objective of the H_∞ controller is to achieve a step response with no overshoot measured at the X-axis position sensor, and at least the same rise time as the PID controller, but with more damping for the structural modes.

Fig. 17 shows the H_∞ controller scheme, with p the X-axis position and a the acceleration of the tool in X-direction. The reference trajectory is specified by p_{ref} and a_{ref}. The signals e_a and e_p are, respectively, the error on the axis position $p - p_{\text{ref}}$ and the tool acceleration error $a - a_{\text{ref}}$. The plant model G is a fourteenth-order representation of the machine dynamics in the nominal position (as depicted in Fig. 15). The controller C, which is to be designed, generates the control signal u (the torque applied to the X-axis motor).

The main advantage of the H_∞ control theory is that it accounts for information on the model uncertainty in the controller design. The knowledge of the dynamic behavior of the machine in its entire operation space allows us to make a well-considered choice for this uncertainty model. Assuming a multiplicative unstructured uncertainty block on the system outputs, the uncertainty consists of the model variation due to the difference between the fourteenth-order control model in its nominal position and the high-order state-space representations of the reduced finite-element models of the machine in its extreme working positions. The robustness weighting functions $W_{r,a}$ and $W_{r,p}$ are low-order transfer functions representing the estimated amplitude of an upper bound of the multiplicative uncertainty. They are the result of a numerical optimization process reducing the surface between them and the envelope of the relative model variations corresponding to the machine in its extreme working positions. Fig. 18 shows these relative model variations and the computed robustness weighting functions $W_{r,a}$ and $W_{r,p}$.

The small-gain theorem [14] states that robust stability can be guaranteed when

$$\left\| \begin{matrix} W_{r,a} T_{aa} \\ W_{r,p} T_{pp} \end{matrix} \right\|_\infty < 1 \tag{1}$$

where T_{aa} and T_{pp} are the transfer functions seen by the uncertainties. For the multiplicative uncertainty being considered here, these are the complementary sensitivity functions: $T = GC/(1+GC)$.

The H_∞ synthesis method also requires the desired performance to be specified in terms of the shape of certain transfer functions. Small tracking errors of the axis can be obtained by requesting the transfer function S_{pp} from reference position p_{ref} to tracking error e_p to be small at low frequencies. In the high-frequency range, this should be relaxed to allow robustness against uncertainty at these frequencies. By forcing the maximum amplitude of the transfer function S_{pa} from reference position p_{ref} to tool acceleration a to be smaller than a certain constant value, the maximum acceleration, excited by the trajectory, is limited. The transfer functions determining the performance S_{pp} and S_{pa} can now be shaped by the following H_∞-norm condition:

$$\left\| \begin{matrix} W_{p,p} S_{pp} \\ W_{p,a} S_{pa} \end{matrix} \right\|_\infty < 1 \tag{2}$$

where $W_{p,p}$ is large at low frequencies (forcing S_{pp} to be small) and small at high frequencies, in order not to conflict with the robustness specifications. The weighting function $W_{p,a}$ is a certain constant value limiting the maximum amplitude of S_{pa}.

The control input amplitude is limited to avoid actuator saturation by weighting the transfer function CS_{pu} from reference position p_{ref} to control signal u with the constant weight W_u by requiring that

$$\|W_u CS_{pu}\|_\infty < 1. \tag{3}$$

The weight W_u is chosen as a very small constant, because no actuator saturation is expected (which has been confirmed by the simulations afterwards). Hence, only the performance and the robustness are traded off, by shaping the sensitivity S and the complementary sensitivity function T, through (1) and (2). The method is therefore called the S/T-mixed sensitivity design.

The control design now aims at finding the controller C that simultaneously minimizes the given specifications (1)–(3) by combining them into one H_∞ norm. When the system and the

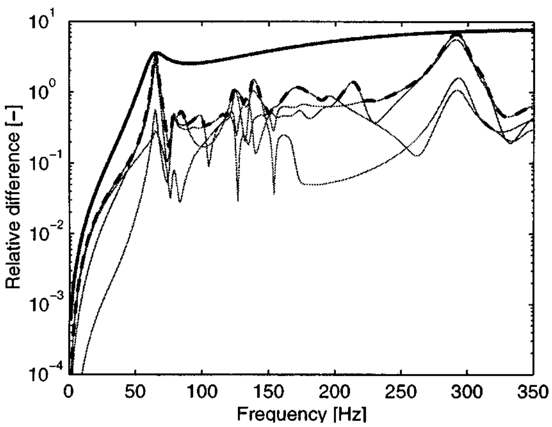

(a)

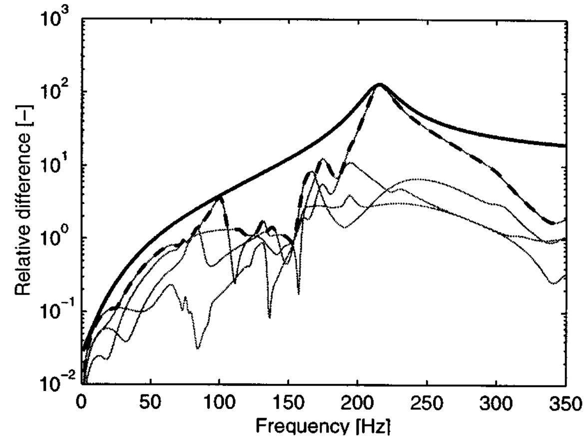

(b)

Fig. 18. Relative model variations (thin line), their envelope (dashed line), and the upper bounds $W_{r,a}$ and $W_{r,p}$ (solid line). (a) For the position output and (b) for the acceleration output.

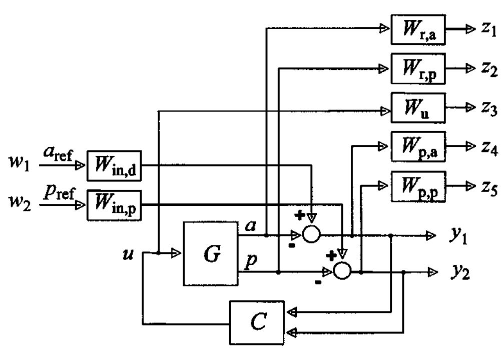

Fig. 19. The H_∞ controller synthesis scheme.

weighting functions are combined as in Fig. 15, the performance specifications (1)–(3) are obtained by the design specification

$$\min_C \|T_{wz}\|_\infty \leq 1 \tag{4}$$

with w the system inputs and z the weighted system outputs.

However, minimizing (4) leads to shaping ten transfer functions, while not all of them are of the same importance. Therefore, weighting functions $W_{\mathrm{in},d}$ and $W_{\mathrm{in},p}$ are added on the inputs to allow to emphasise certain transfer functions more than others. The weighting functions are determined iteratively through simulation. The procedure is described in detail in [15].

Implementation of the obtained controller on the high-order model of the machine in its nominal position results in the step response of Fig. 20.

The position response at the tool (on the left-hand side) stays within 1% of the desired value after 50 ms with the H_∞ controller, while it takes more than 150 ms with the PID controller. The amplitude of the tool acceleration (on the right hand) is also significantly smaller with the H_∞ controller than with the PID controller. Fig. 21(a) shows the assembled finite-element model of the machine in its nominal configuration. Intuitively, the largest difference with this nominal machine configuration is expected to occur when all slides are in the extreme positions, as shown in Fig. 21(b). The implementation of the same H_∞ controller on the high-order model of the machine in this extreme configuration yields the step response of Fig. 22. Despite the tremendous difference between this machine model and the nominal model, the H_∞ controller remains stable and performs very well. Its settling time is again much shorter, and the vibrations at the tool decay faster than with the PID controller.

However, although the acceleration of the tool caused by the motion of the machine tool is decreased, simulations show that there is no decrease for the accelerations caused by cutting forces. The reason is that H_∞ synthesis aims at changing the shape of the transfer functions in the cost function $\|T_{wz}\|_\infty$ and not the overall system closed-loop behavior. The H_∞ synthesis therefore introduces controller zeroes at the system poles and vice versa. In order to overcome this severe drawback of the S/T-mixed sensitivity design, Van den Braembussche [15] introduced an alternative H_∞-controller based on an $S/GS/CS/T$-mixed sensitivity approach. This alternative H_∞-controller yields a better disturbance rejection at the tool, at the expense of a slightly reduced performance. However, based on the observation that the internal collocated velocity feedback loop of the PID controller inherently adds damping to the system, a much better solution is obtained by building the previously developed H_∞ controller around the machine model with the PI-velocity loop already closed. The step responses of this modified H_∞ controller are similar to those obtained with the original H_∞ controller (represented in Figs. 20 and 22), while its disturbance rejection capability at the tool is similar to that of the PID controller. This latter quality is illustrated in Fig. 23, which shows the frequency response function from a force applied at the tool to the tool acceleration for the machine in its nominal configuration, without controller, with the PID controller, and with the modified H_∞ controller. The curve corresponding to the original H_∞ controller exactly coincides with the curve corresponding to the machine without controller.

V. Closing Remarks

In this paper, elements of a virtual engineering environment or mechatronic compiler for designing mechatronic systems

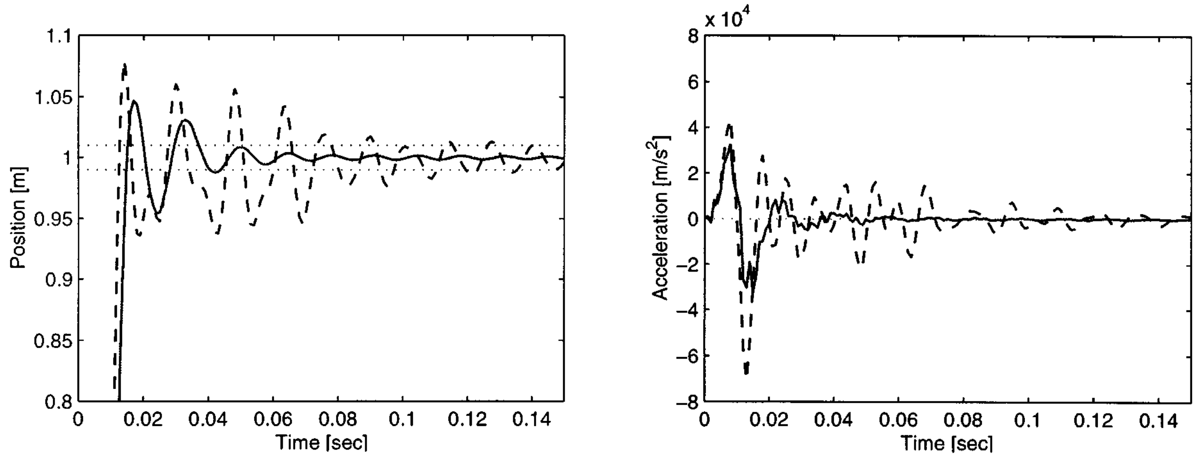

(a) (b)

Fig. 20. Step response at the tool of the machine in its nominal configuration, with the H_∞ controller (solid line) and with the PID controller (dashed line). (a) Position response and (b) acceleration response.

(a) (b)

Fig. 21. Assembled finite-element model (a) in its nominal configuration and (b) in the extreme configuration (right).

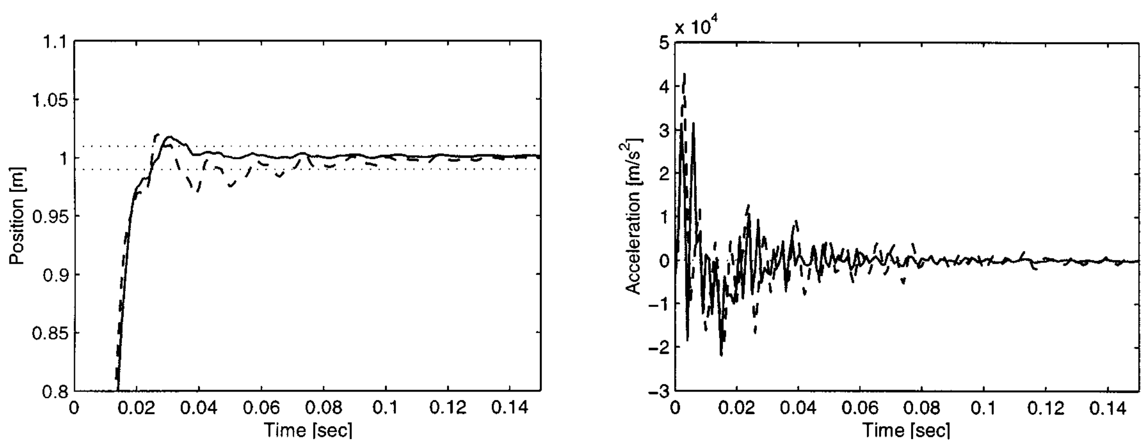

(a) (b)

Fig. 22. Step response at the tool of the machine in its nominal configuration, with the H_∞ controller (solid line) and with the PID controller. (a) Position response and (b) acceleration response.

have been presented. This paper is built around the example of a three-axis machine tool. In a first step, genetic algorithms are used to determine, in the conceptual design phase, the configuration that optimally satisfies one or more design requirements, like maximal static stiffness, high dynamic stiffness, maximal working space, etc. Subsequently, this optimal concept can be worked out in a detailed design step by machine design specialists (this step is not described in the paper). Finally, in a concurrent engineering step, the mechanical design and the controller are simultaneously optimized. This requires the construction of a mechanical machine model in its different configurations. This step has been worked out using the component synthesis method. A robust controller, e.g., an H_∞ or sliding-mode controller, can be designed such that robust

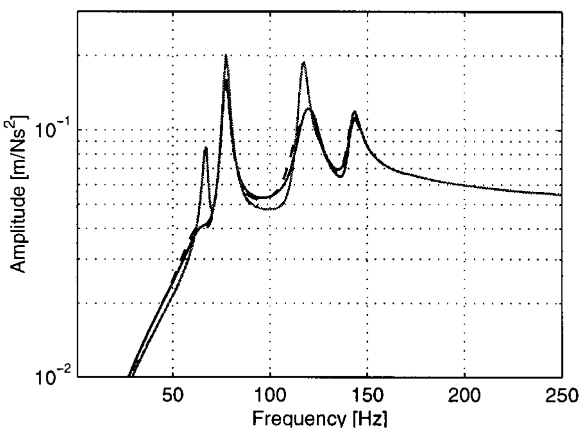

Fig. 23. Transfer function from the force at the tool to the tool acceleration for the machine in its nominal configuration, without controller (gray line), with the PID controller (dashed line), and with the modified H_∞ controller (black line).

performance is obtained for all configurations. Work is still under way in which mechanical design modifications are also included in the overall optimization of the controller.

REFERENCES

[1] H. Van Brussel, "Mechatronics—A powerful concurrent engineering framework," *IEEE/ASME Trans. Mechatron.*, vol. 1, no. 2, pp. 127–136, 1996.

[2] A. Lipóth, "Systematic creation and evaluation of the global structures of machining centres," doctoral dissertation, Department of Manufacturing Engineering, Technical Univ. of Budapest, 1993. (in Hungarian).

[3] *Multibody Systems Handbook*, W. Schiehlen, Ed., Springer-Verlag, Berlin, 1989, pp. 246–264. "ROBOTRAN".

[4] D. E. Goldberg, *Genetic Algorithms in Search, Optimisation, and Machine Learning*. Reading, MA: Addison-Wesley, 1989.

[5] M. Wall, *A C++ Library of Genetic Algorithm Components*. Cambridge: Mechanical Engineering Department, Massachusetts Institute of Technology, 1996. GAlib Version 2.4.

[6] R. R. Craig, "A review of time-domain and frequency-domain component-mode synthesis methods," *Int. J. Anal. Exp. Modal Anal.*, vol. 2, no. 2, pp. 59–72, 1987.

[7] P. De Fonseca, D. Vandepitte, H. Van Brussel, and P. Sas, "Dynamic model reduction of a flexible three-axis milling machine," in *Proc. 23rd International Noise and Vibration Engineering Conf. (ISMA 23)*, vol. I, Leuven, 1998, pp. 185–194.

[8] W. Heylen, S. Lammens, and P. Sas, *Modal Analysis: Theory and Testing*, Leuven, Belgium: K. U. Leuven, 1995.

[9] R. M. Hintz, "Analytical methods in component modal synthesis," *AIAA J.*, vol. 13, no. 8, pp. 1007–1016, 1975.

[10] T. Rose, "Component modal synthesis for coupled dynamic analysis using superelements," MacNeal-Schwendler Corporation, MSC internal paper, 1996.

[11] G. Bianchi, F. Paolucci, P. Van den Braembussche, and H. Van Brussel, "Toward virtual engineering in machine tool design," *Ann. CIRP*, vol. 45, no. 1, 1996.

[12] H. R. Cannon and E. Schmitz, "Initial experiments on the end-point control of a flexible one-link robot," *Int. J. Robot. Res.*, vol. 3, no. 3, pp. 62–75, 1984.

[13] H. Van Brussel, J. De Schutter, D. Torfs, C. H. Chen, and J. Swevers, "Accurate and robust tracking control of flexible mechatronic systems," in *Proc. Eur. Control Conf.*, Groningen, the Netherlands, 1993, pp. 2260–2265.

[14] K. Zhou, J. C. Doyle, and K. Glover, *Robust and Optimal Control*. Englewood Cliffs, NJ: Prentice-Hall, 1995.

[15] P. Van den Braembussche, "Robust Motion Control of Machine Tools with Linear Motors," Ph.D. dissertation, K. U. Leuven, Leuven, Belgium, 1998.

Hendrik Van Brussel (S'68–M'68–SM'85–F'95) was born in 1944. He received the B.Sc. ME (Technisch Ingenieur) degree from Hoger Technisch Instituut, Oostende, Belgium, in 1965 and the M.Sc. EE (Burgerlijk Ingenieur) and Ph.D. degrees from Katholieke Universiteit (K. U.) Leuven, Belgium, in 1968 and 1971, respectively.

He is a full Professor in mechatronics and automation with the Faculty of Engineering, K. U. Leuven, and Chairman of its Department of Mechanical Engineering. From 1971 until 1973, he was active in Bandung, Indonesia, establishing a Metal Industries Development Centre and working as an Associate Professor at the Institut Teknologi Bandung. He was a pioneer in robotics research in Europe and an active promoter of the mechatronics idea as a new paradigm in machine design. He has published more than 200 papers on different aspects of robotics, mechatronics, and flexible automation. His present research interest is shifting toward holonic manufacturing systems, behavior-based robots, and micro and precision engineering, including microrobotics. He is President of CIRP (International Institution for Production Engineering Research).

Prof. Van Brussel is a Fellow of SME and a member of the Royal Flemish Academy of Belgium for Sciences and Fine Arts. He received an honorary doctor degree from the Politehnica University in Bucarest, Romania, and from Rheinisch-Westfälische Technische Hochschule, Aachen, Germany, in 1994.

Paul Sas received the mechanical engineer degree and the Ph.D. degree in mechanical engineering from Katholieke Universiteit (K. U.) Leuven, Belgium, in 1976 and 1982, respectively.

In 1984, he became a Senior Researcher at K. U. Leuven funded by the National Scientific Research Fund of Belgium (mechanical engineering). At the same university he became a Lecturer in 1985, Associate Professor in 1988, Professor in 1992, and full Professor in 1997. He teaches courses in mechanical vibrations, structural dynamics, machine design, and safety mechanics. He is currently Chairman of the division PMA of the Mechanical Engineering Department of K. U. Leuven and Head of the Noise and Vibration Research Group of the same division. He is an author or coauthor of more than 100 papers on noise and vibration measurements and analysis, model updating, noise source identification, active noise, and vibration control. Since 1988, he has been Chairman of the biennial international ISMA conference on Numerical and Experimental Techniques in Structural Dynamics and Director of the yearly ISMA short courses on Modal Analysis and Numerical Methods in Vibro-Acoustics. He is a Reviewer for a number of international journals. Since 1985, he has been involved in several international research projects on noise and vibration analysis, most of them in collaboration with leading European automotive industries (EC/Brite-Euram, EC/Esprit, and ESA). In 1979, he was a Cofounder of Leuven Measurement and Systems.

Prof. Sas is a member of ASA, ABAV, SBM, KVIV, SEM, and VDI. He is a laureate of the Royal Academy for Sciences, Literature and Arts of Belgium (1984).

István Németh was born in 1967. He received the M.Sc. degree in mechanical engineering from the Technical University of Budapest (TUB), Hungary, in 1991. He is currently pursuing the Ph.D. degree at the Katholieke University Leuven.

From 1991 to 1993, he was a Quality Assurance Engineer with GE Lighting-Tungsram, Budapest. His doctoral dissertation is on conceptual design of three-axis machine tools.

Pierre De Fonseca was born in Deinze, Belgium, in 1971. He received the degree in mechanical engineering and the Ph.D. degree from the Katholieke Universiteit (K. U.) Leuven, Belgium, in 1995 and 2000, respectively.

His research interests include mechatronics, integrated structure/control design, active noise and vibration control, and optimization.

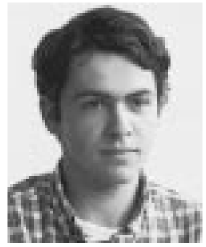

Pieter Van den Braembussche received the engineering degree and the Ph.D. degree from the Katholieke Universiteit (K. U.) Leuven, Belgium, in 1992 and 1998, respectively, both in mechanical engineering.

From 1992 to 1998, he has been a Research Assistant at the K. U. Leuven in the field of motion and vibration control with emphasis on motion control of high-performance machine tools with linear motors. In 1998, he joined Verhaert Design and Development, with responsibility for the Attitude Control and Navigation System of the PROBA satellite, which is developed for the European Space Agency.